

## Mathematical modeling and simulation of gel drying with supercritical carbon dioxide

ALEKSANDAR ORLOVIĆ<sup>\*#</sup>, STOJAN PETROVIĆ<sup>#</sup> and DEJAN SKALA

*Faculty of Technology and Metallurgy, University Belgrade, Karnegijeva 4, P. O. Box 3503,  
11120 Belgrade, Serbia and Montenegro (e-mail: orlovic@tmf.bg.ac.yu)*

(Received 30 June 2003, revised 6 July 2004)

*Abstract:* Mathematical models of alumina/silica gel supercritical drying with carbon dioxide were studied using supercritical drying experimental data. An alumina/silica gel with zinc chloride was synthesized and dried with supercritical carbon dioxide, and its weight change was monitored as a function of drying time. The pore size distribution of the obtained aerogel was determined using the BET method and nitrogen adsorption/desorption. The mathematical model of the supercritical drying of the wet gel was represented as unsteady and one-dimensional diffusion of solvent through the aerogel pores filled with supercritical carbon dioxide. Parallel pore model and pores in series model were developed on the basis of the measured porous structure of the aerogel. It was found that these models which use different effective diffusivity value for each pore size were in much better agreement with the experimental data than models which use an overall effective diffusivity. The local effective diffusivity coefficients were calculated using different tortuosity values for each pore size, and they were distributed according to the pore size distribution data. Model simulations of the supercritical drying with carbon dioxide confirmed that the drying temperature and gel particle diameter have a significant influence on the drying time.

*Keywords:* supercritical drying, aerogels, modeling of diffusion.

### INTRODUCTION

After dissolution of the reactants in an appropriate solvent and subsequent gelation of the sol, the formed wet gel can be dried by several methods. When elevated temperature and atmospheric pressure or vacuum are applied, the presence of two phases (a liquid and a vapor one) leads to the evolution of capillary pressure in the gel pores. Consequently, cracks occur in the gel network, changing its original structure. The obtained material is known as a xerogel. Another available drying method is the evacuation of the solvent using supercritical drying, which produces an aerogel.<sup>1,2</sup> The solvent and sol-gel reaction by-products present in the gel pores

\* Corresponding author.

# Serbian Chemical Society active member.

are evacuated at a temperature and a pressure higher than the critical temperature and pressure of the solvent (or their mixture), or by another supercritical extracting fluid with moderate values of critical parameters (commonly carbon dioxide). Using the supercritical drying method, the evolution of the capillary pressure is avoided and the original gel structure remains largely preserved.<sup>3,4</sup> Aerogels are usually described as open structure materials, typically highly porous, with low particle sizes and large surface areas. Some potential fields of aerogels applications are: optoelectronics, special technical ceramics, thermal insulation and heterogeneous catalysis.

Since the supercritical drying procedure is the most complex and time consuming step in the processing of aerogels, mathematical modeling of the supercritical drying procedure could provide important information about scale-up and process optimization. Mathematical models of the extraction of etheric oils from herbal material with supercritical carbon dioxide,<sup>5–10</sup> and of the extraction of heavy organic compounds from polluted soil with supercritical carbon dioxide<sup>11–13</sup> (polluted soil remediation), are well described in the literature. On the other hand, to the best of our knowledge, mathematical models describing wet gel drying with supercritical carbon dioxide are rare and oversimplified.<sup>14–16</sup>

In this paper, mathematical modeling of wet gel drying with supercritical carbon dioxide is presented. An alumina/silica gel with zinc chloride investigated as the alkylation catalyst<sup>17,18</sup> was obtained in a one step sol-gel synthesis with 1-butanol as the solvent. The obtained wet gel was dried with supercritical carbon dioxide and the change of gel weight was monitored in time. The porous structure of the aerogel was analyzed using the BET method with nitrogen as the adsorbent at 77 K. The model equations were solved using the finite difference method and a FORTRAN program.

#### EXPERIMENTAL

The sol-gel synthesis was performed according to Miller *et al.*<sup>19</sup> Aluminum tri-sec-butoxide (9.84 g, 0.04 mol) was mixed with 1-butanol (100 cm<sup>3</sup>) and then TEOS (8.32 g, 0.04 mol) was added. The mixture was stirred vigorously and heated to 343 K for 5 min until a clear solution was obtained, after which the solution was cooled down to room temperature. Then, it was hydrolyzed with water (18.75 cm<sup>3</sup>, 1.04 mol) in which zinc chloride (3.75 g, 0.025 mol) had already been dissolved. The solution was stirred for 15 min and left to stand overnight (gelation). The obtained gel was a viscous liquid (particulate gel), containing: 1-butanol (solvent), ethanol (product of TEOS hydrolysis) and water. Prior to supercritical drying with carbon dioxide it was necessary to remove the water, ethanol and a part of the 1-butanol by heating the gel to 423 K (in order to preserve only 1-butanol presence and diffusion through the aerogel porous structure). A glass cylinder (open at one end) was filled with wet gel (the gel cylinder dimensions were: 11 mm height and 11 mm diameter). The wet gel sample was then placed in a 70 cm<sup>3</sup> tubular extractor (Autoclave Engineers Supercritical Extraction Screening System), and filled with liquid carbon dioxide from a storage cylinder. The pressure was then raised above the critical one (74 bar) at room temperature. After reaching 80 bar, the temperature was increased to 313 K. When the desired drying conditions were reached (100 bar and 313 K), supercritical carbon dioxide flow through the extractor was started. After 30 min,

the flow was stopped, the pressure was released from the system (at 313 K in order to avoid two phases of carbon dioxide), and the sample was removed from the extractor. After recording the sample weight, the above described procedure was repeated at regular time intervals. The total consumption of carbon dioxide was recorded for each drying time interval. The experimental data obtained using the above described procedure, are shown in Fig. 1.

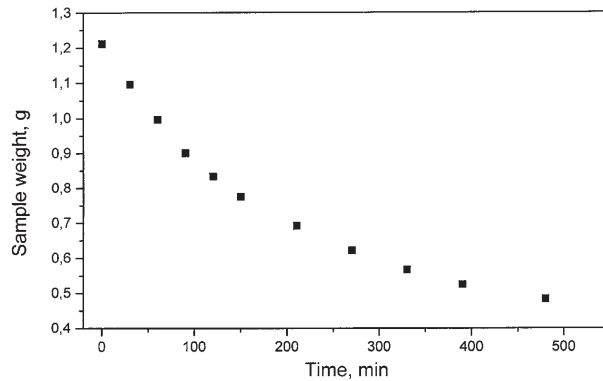


Fig. 1. Experimental data of the gel cylinder drying.

The aerogel weight change with drying time is the result of unsteady, one-dimensional and unidirectional diffusion of 1-butanol (solvent) through aerogel pores filled with supercritical carbon dioxide. Since the aerogel porous structure is the key parameter which determines the supercritical drying dynamics, the BET method using nitrogen adsorption/desorption at 77 K was used to obtain the pore size distribution of the dry aerogel. The adsorption and desorption isotherms are shown in Fig. 2, and the pore size distribution plot (calculated using the BJH method) is shown in Fig. 3. The specific surface area and total pore volume determined from the BET measurements were 175.63 m<sup>2</sup>/g and 1.04 cm<sup>3</sup>/g, respectively. After completion of the supercritical drying experiment, cracks were observed in the dry aerogel cylinder. This was to be expected since the wet aerogel was constrained in a glass cylinder. The volume of macropores was calculated from the difference between the volume of the removed 1-butanol (calculated from the total aerogel weight change after drying and the 1-butanol density at 298 K) and the total pore volume measured using the BET method (micro and mesopores). The distribution of the pore volumes is shown in Table I.

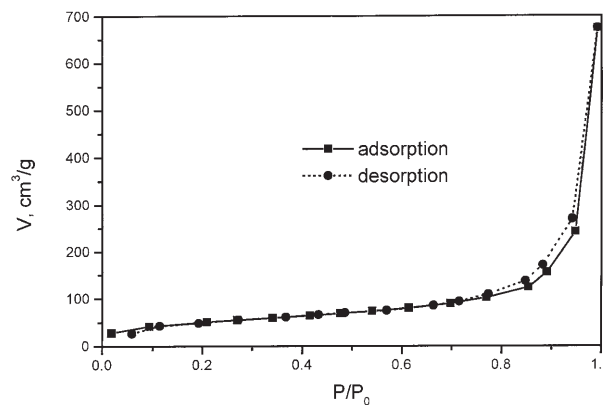


Fig. 2. Adsorption/desorption isotherms of the aerogel.

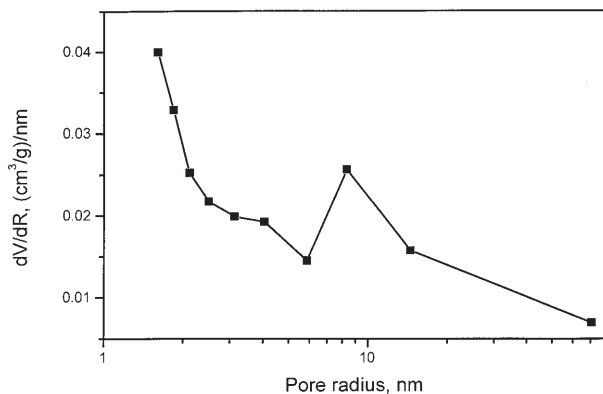


Fig. 3. Pore size distribution of the aerogel.

TABLE I. Pore radius, pore volume distribution, solvent weight distribution, and local pore tortuosity of the aerogel

Pore radius/ $10^{-10}$ m	Pore volume/ $\text{cm}^3 \text{g}^{-1}$	1-Butanol weight/g	Pore tortuosity
> 705	0.8210	0.3214	2.50
705.08	0.7105	0.2870	3.00
144.06	0.1550	0.0607	3.20
83.05	0.0595	0.0233	3.55
58.59	0.0359	0.0140	3.90
40.45	0.0202	0.0079	4.25
31.15	0.0150	0.0059	4.60
24.95	0.0097	0.0038	4.95
21.11	0.0075	0.0029	5.30
18.38	0.0076	0.0030	5.65
15.98	0.0039	0.0036	6.00

#### MATHEMATICAL MODEL

Equation (1) represents the mathematical model of unsteady and one-dimensional diffusion through a porous solid and it can describe the gel drying process, since the solution of 1-butanol in carbon dioxide is highly diluted.

$$\frac{\partial C}{\partial t} = D_{\text{eff}} \frac{\partial^2 C}{\partial x^2} \quad (1)$$

The initial and boundary conditions are given as follows:

– initial conditions  $t = 0, x = 0 \Rightarrow C = C^*$ ;  $0 < x \leq L \Rightarrow C = C^0$

– boundary conditions  $t > 0, x = 0 \Rightarrow C = C^i$

$t > 0, x = L \Rightarrow \frac{\partial c}{\partial x} = 0$ .

The diffusion resistance of the supercritical carbon dioxide film above the aerogel cylinder was neglected, and the 1-butanol concentration at the interface was taken to be equal to the 1-butanol concentration in the bulk supercritical carbon dioxide. The validity of this assumption was confirmed by the two orders of magnitude difference between the solubility of 1-butanol in supercritical carbon dioxide at 100 bar and 313 K, and the calculated average concentration of 1-butanol in the supercritical carbon dioxide during our experiment. The solubility of 1-butanol in supercritical carbon dioxide ( $y_{\text{Bu-OH}} = 0.0135$ ) was obtained using CHEMSHARE DESIGN II computer software (Pend-Robinson equation of state) and literature data.<sup>20</sup> Since supercritical drying does not promote the collapse of the gel network, the wet and partially wet gel porous structure was approximated with the dry aerogel porous structure<sup>2</sup> (Table I). The above partial differential equation with initial and boundary conditions was solved numerically using the finite difference method.<sup>21</sup>

The most important parameter of the mathematical model is the effective diffusivity of 1-butanol through the aerogel pores filled with supercritical carbon dioxide. The effective diffusivity was calculated using the binary diffusivity coefficient, material overall porosity, constriction factor and tortuosity, as shown in Eq. (2).

$$D_{\text{eff}} = \frac{D_{\text{AB}} \varepsilon_p \sigma}{\tau} \quad (2)$$

For solids containing micropores, Knudsen diffusivity can play an important role, and in this case the overall effective diffusivity can be calculated using Eq. (3)

$$\frac{1}{D_{\text{eff}}} = \frac{\tau}{D_{\text{AB}} \varepsilon_p \sigma} + \frac{1}{D_{\text{K}}} \quad (3)$$

The binary diffusivity (1-butanol – carbon dioxide) at normal pressure and drying temperature was calculated using the Fuller, Schettler and Giddings empirical correlation<sup>22</sup> (Eq. (4)). The value of the binary diffusivity at normal pressure was used to calculate the binary diffusivity at the supercritical drying pressure, using the Takahashi correlation<sup>22</sup> (Eq. (5)):

$$D_{\text{AB}} = \frac{10^{-3} T^{1.75} [(M_{\text{A}} + M_{\text{B}}) / M_{\text{A}} M_{\text{B}}]^{1/2}}{P [(\Sigma \nu)_{\text{A}}^{1/3} + (\Sigma \nu)_{\text{B}}^{1/3}]^2} \quad (4)$$

$$\frac{D_{\text{AB}} P}{(D_{\text{AB}} P)^+} = f(T_{\text{r}}, P_{\text{r}}) \quad (5)$$

The Knudsen diffusivity<sup>23</sup> was calculated using Equation 6:

$$D_{\text{K}} = \Psi \frac{2}{3} r_p \sqrt{\frac{8RT}{\pi M_i}} \quad (6)$$

Based on the method of the calculation of the effective diffusivity, four different models were developed. In the shrinking core model (SCM1), the effective diffusivity calculated by Eq. (2) was used. The binary diffusivity at the supercritical drying pressure and temperature was calculated using Eqs. (4) and (5), the constriction factor was assumed to be 1, the porosity was taken as the overall porosity including macropores, and tortuosity values of 1.5 and 3 were used (commonly used values for porous catalytic materials). The model results obtained using the SCM1 procedure are shown in Figure 4. In the second shrinking core model (SCM2), it was assumed that Knudsen diffusivity plays an important role, and the effective diffusivity was calculated using Eq. (3). In this model, the binary diffusivity at the supercritical drying pressure and temperature was calculated using Eqs. (4) and (5), the constriction factor was assumed to be 1, the porosity was taken as the overall porosity including macropores, a tortuosity value of 3 was used and the Knudsen diffusivity was calculated using Eq. (6) with an average pore radius of  $29.6 \times 10^{-10}$  m and  $\psi = 1$ . The resulting drying plot obtained using the SCM2 is shown in Fig. 4.

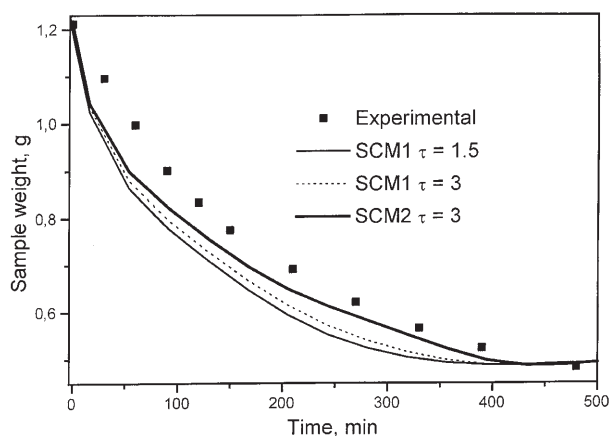


Fig. 4. Comparison of model results and experimental data using the SCM1 and SCM2.

The parallel pore model (PPM) and pores in series model (PSM)<sup>24</sup> were developed using the pore size distribution data. Schematic representations of the idealized aerogel porous structure used to approximate the actual aerogel porous structure are shown in: Fig. 5A for the PPM and Fig. 5B for the PSM (both Figures demonstrate the case of a partially dried gel). The basic assumptions of the parallel pore model (PPM) are: pores with different dimensions are distributed in parallel order, they are all being dried simultaneously, and all pore sizes are in contact with supercritical carbon dioxide at all time intervals. In the PPM the effective diffusivities of the mesopores and macropores were calculated using Equation (2) with the use of different tortuosity values for each pore size (Table I) and the effective diffusivity of the micropores was calculated as the Knudsen diffusivity with a micropore average pore radius of  $4.16 \times 10^{-10}$  m and  $\psi = 1$ . The set of tortuosity values was established by

adjusting the values to fit the experimental data and using following assumptions: typical tortuosity values for alumina/silica materials are in the range of 2 – 6<sup>24,25</sup> and smaller size pores are more tortuous than bigger ones (since they are more irregularly shaped as a consequence of the gel network growing process). The concentration gradients of the solvent in the gel pores filled with supercritical carbon dioxide were calculated using Equation (1) in the finite difference form (for each pore size with different effective diffusivity values). When  $C$  reached the value of  $C^*$ , a location of the liquid – supercritical fluid interface was established for each pore size and after each time interval (by the interpolation method). Since the liquid – supercritical fluid interface was moving through the pores in time, the sample weight change as a function of time was calculated by summarizing the contributions of the weight change for all pore sizes at each time increment according to Eq. (7)

$$\Delta m|_{\Delta t} = \sum_{i=1}^N (V_i|_{t_j} - V_j|_{t_{i-1}}) \rho_{\text{solv}} \quad (7)$$

The tortuosity values shown in Table I were also used in the pores in series model (PSM). In this model (Figure 5B) pores of different sizes are arranged in series stretching through the material. Larger radius pores are dried first, and as they empty the next pore size comes in contact with supercritical carbon dioxide and their drying commences. This continues from one pore size to another until the smallest pores are emptied and the sample is dry. In the PSM the effective diffusivities of the mesopores and macropores were calculated from Eq. (2) with the use of different values of tortuosity for each pore size (Table I) and the effective diffusivity of the micropores was calculated as the Knudsen diffusivity with a

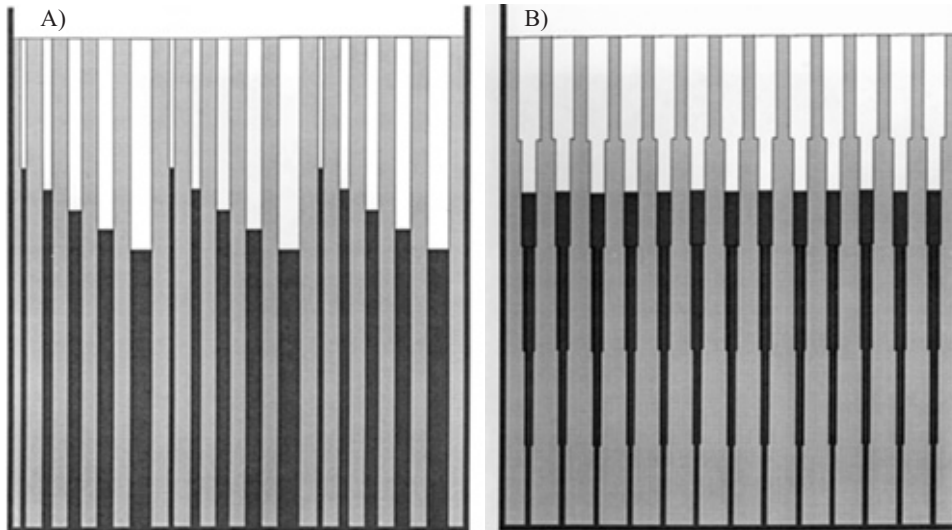


Fig. 5. Schematic representation of the porous structure of the aerogel (case of partially dried gel is depicted): A – parallel pore model and B – pores in series model.

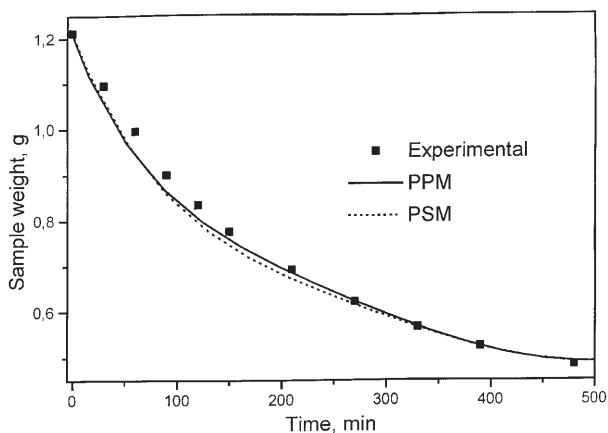


Fig. 6. Comparison of model results and experimental data using the PPM and PSM.

micropore average pore radius of  $4.16 \times 10^{-10}$  m and  $\psi = 1$ . As in the case of the PPM, the concentration gradient in the pores was used to establish the supercritical fluid – liquid interface at each time interval (by the interpolation method). The weight change between the time intervals was then calculated using Eq. (8). The resulting drying plots obtained using the PPM and PSM are shown in Fig. 6.

$$\Delta m|_{\Delta t} = (V|_{t_j} - V|_{t_{j-1}})\rho_{\text{solv}} \quad (8)$$

The shrinking core model SCM1, which uses one value of the effective diffusivity for the whole material, fails to predict the experimental data well. The main reason for the poor accuracy of this model is the application of one mean value of effective diffusivity for a material with a broad pore size distribution. The accuracy of the second shrinking core model SCM2, which also uses one value of the effective diffusivity for the whole material, is improved in comparison with the SCM1. The main reason for the improved accuracy lies in the reduced effective diffusivity, due to the incorporation of the Knudsen diffusivity in overall effective diffusivity. The best fits of the experimental data are achieved using the PPM and PSM, although the former is slightly better. These models use idealized representations of the aerogel porous structure but incorporation of localized values of the effective diffusivity results in improved model accuracy. Although the tortuosities used in the PPM and PSM seem somewhat high, values similar to these<sup>24</sup> or even larger ones<sup>26</sup> are reported in the literature. Even the PPM and PSM models fail to predict with high accuracy the upper part of the experimental drying curve. This is probably due to the slightly higher value of the estimated 1-butanol solubility in supercritical carbon dioxide. However, the considerably better agreement of the PPM and PSM results in comparison to the SCM results confirms the advantage of using local effective diffusivity values when simulating the supercritical drying process of a material with broad pore size distribution (as in the case of an alumina/silica aerogel).



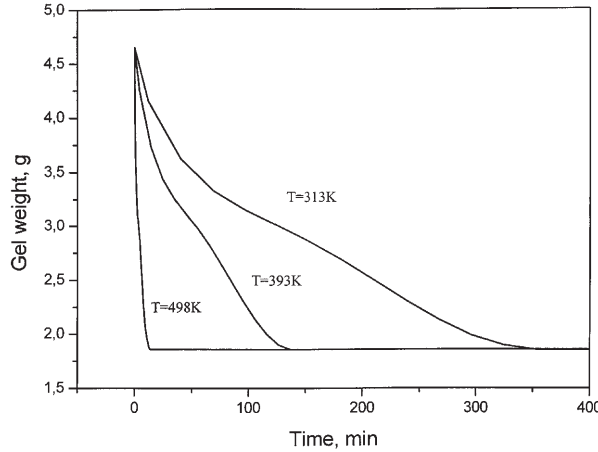


Fig. 7. Supercritical drying simulation of a gel sphere ( $R_s = 1.0$  cm) at different temperatures.

The most important process parameters influencing the dynamics of supercritical drying with carbon dioxide are: the solubility of the solvent in the supercritical carbon dioxide (effect of temperature and pressure) and the dimensions of the wet gel body. In order to study the influence of these process parameters, a simulation of the drying of wet spherical gel particles of different diameters and at different temperatures was performed. The results were obtained by solving Eq. (9) using the finite difference method and the PPM model:

$$\frac{\partial C}{\partial t} = D_{\text{eff}} \frac{1}{r^2} \left[ \frac{\partial}{\partial r} \left( r^2 \frac{\partial C}{\partial r} \right) \right] \quad (9)$$

with initial and boundary conditions:

- initial conditions  $t = 0, r = R_s \Rightarrow C = C^*$ ;  $0 \leq r < R_s \leq C = C^0$
- boundary conditions  $t > 0, r = 0 \Rightarrow \frac{\partial C}{\partial r} = 0$
- $t > 0, r = R_s \Rightarrow C = C^i$

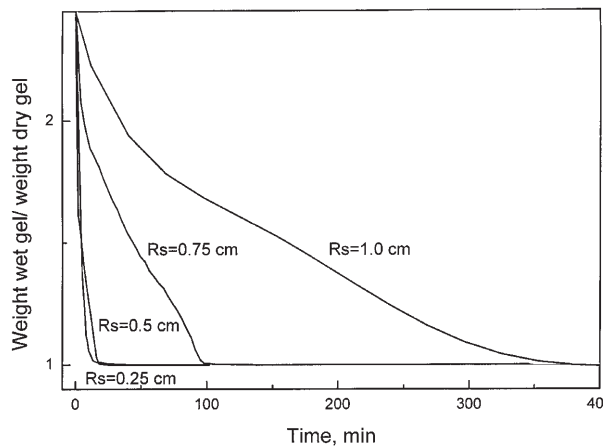


Fig. 8. Supercritical drying simulation using different spherical dimensions at 313 K.

The simulation results of gel drying at 313 K, 393 K and 498 K are shown in Fig. 7. The solubility of 1-butanol in supercritical carbon dioxide at 100 bar was determined using CHEMSHARE DESIGN II software and the Peng-Robinson equation of state ( $y_{\text{BuOH}} = 0.0356$  at 393 K and  $y_{\text{BuOH}} = 0.312$  at 498 K). As a consequence of the increased solubility of 1-butanol at elevated temperatures, the drying time is decreased considerably. The influence of particle dimension on the dynamics of supercritical drying is demonstrated in Fig. 8. As expected, larger diameter spheres need longer drying times, but it is interesting to note that 5 h of supercritical drying is needed to completely dry bodies of moderate dimensions (1 cm radius sphere). The optimal supercritical drying procedure should therefore include the minimum characteristic dimension of the drying body and the highest possible drying temperature.

#### CONCLUSION

In order to investigate supercritical drying as the most complex and time consuming step in the processing of aerogels, a mathematical model based on the porous structure of an aerogel was developed. Alumina/silica aerogel was obtained using a one step sol-gel synthesis and subsequent drying with supercritical carbon dioxide. The wet gel weight change with time was monitored during a supercritical drying procedure and the dry aerogel sample porous structure was determined using the BET method using nitrogen adsorption/desorption. The mathematical model of the supercritical drying of a wet gel sample was represented as unsteady and one-dimensional diffusion of 1-butanol through the aerogel pores filled with supercritical carbon dioxide. Four different procedures for calculating the effective diffusivity as the most important model parameter were developed. The shrinking core models use one value of the effective diffusivity for the whole material, and they fail to describe the drying experiment accurately. The parallel pore model and the pores in series model, which were developed on the basis of the measured aerogel porous structure, use a different effective diffusivity value for each pore size (with a local tortuosity value for each pore size), and their agreement with the experimental supercritical drying data is much better, than those of the shrinking core models. Simulations of supercritical drying with carbon dioxide using the parallel pore model, demonstrated the significant influence of the drying temperature and the dimensions of the wet gel particles on the dynamics of supercritical drying. These simulations indicate that a significant reduction of the drying time could be achieved by employing minimum particle dimensions of the gel to be dried and the maximum drying temperature.

#### LIST OF SYMBOLS

$C$  – 1-Butanol concentration in supercritical carbon dioxide contained within the aerogel pores, kmol/kmol

$C^*$  – Solubility of 1-butanol in supercritical carbon dioxide, kmol/kmol

- $C^i$  – Concentration at the particle solid/fluid interface, kmol/kmol  
 $C^o$  – Initial concentration of 1-butanol in the aerogel pores, kmol/kmol  
 $D_{AB}$  – Diffusivity of 1-butanol in supercritical carbon dioxide, m<sup>2</sup>/s  
 $D_K$  – Knudsen diffusivity, m<sup>2</sup>/s  
 $D_{eff}$  – Effective diffusivity, m<sup>2</sup>/s  
 $L$  – Length of wet gel cylinder, m  
 $M$  – Molecular weight, kg/kmol  
 $\Delta m|_{\Delta t}$  – Differential weight change of the wet gel cylinder at  $\Delta t$ , kg  
 $N$  – Number of different pore dimensions  
 $P$  – Pressure, bar  
 $r$  – Radial distance, m  
 $r_p$  – Pore radius, m  
 $R$  – Gas constant, kJ/kmol K  
 $R_s$  – Radius of spherical gel particle, m  
 $t$  – Time, min  
 $T$  – Temperature, K  
 $V_{i|j}$  – Volume of  $i^{\text{th}}$  pore filled with 1-butanol at  $j^{\text{th}}$  time increment, m<sup>3</sup>  
 $V_{i|j-1}$  – Volume of  $i^{\text{th}}$  pore filled with 1-butanol at  $(j-1)^{\text{th}}$  time increment, m<sup>3</sup>  
 $V_{|j}$  – Volume of pore (pores in series Fig. 5B) filled with 1-butanol at  $j^{\text{th}}$  time increment, m<sup>3</sup>  
 $V_{|j-1}$  – Volume of pore (pores in series Fig. 5B) filled with 1-butanol at  $(j-1)^{\text{th}}$  time increment, m<sup>3</sup>  
 $x$  – Axial distance, m
- Greek letters  
 $\varepsilon_p$  – Porosity  
 $\Sigma v_i$  – Molecular diffusion volumes in the Fuller, Schettler and Giddings correlation  
 $\sigma$  – Constriction factor  
 $\rho_{\text{solv}}$  – Density of 1-butanol, kg/m<sup>3</sup>  
 $\tau$  – Tortuosity  
 $\psi$  – Geometric constant of the solid

## ИЗВОД

МАТЕМАТИЧКО МОДЕЛОВАЊЕ И СИМУЛАЦИЈА СУШЕЊА ГЕЛА СА  
НАТКРИТИЧНИМ УГЉЕН-ДИОКСИДОМ

АЛЕКСАНДАР ОРЛОВИЋ, СТОЈАН ПЕТРОВИЋ и ДЕЈАН СКАЛА

*Технолошко-металуршки факултет, Универзитет у Београду, Карнегијева 4, п. бр. 3503, 11120 Београд*

У овом раду су испитани математички модели сушења алумосиликатног гела са наткритичним угљен-диоксидом на основу експерименталних података наткритичног сушења. Синтетизовани алумосиликатни гел са цинк-хлоридом је сушен са наткритичним угљен диоксидом, при чему је праћена његова промена масе са временом. Расподела величина пора аерогела је одређена ВЕТ методом и адсорпцијом/десорпцијом азота. Математички модел наткритичног сушења је приказан као нестационарна једнодимензиона дифузија растварача кроз поре аерогела испуњене наткритичним угљен-диоксидом. Модел паралелних пора и модел редно везаних пора су развијени на основу измерене порозне структуре добијеног аерогела. Резултати указују да је слагање модела паралелних пора и модела редно везаних пора са различитим вредностима ефективне дифузивности за поре различитих величина и експерименталних података,

знатно боље него у случају модела који користе једну вредност ефективне дифузивности. Коефицијенти ефективне дифузивности су добијени коришћењем различитих вредности локалних изувијаности пора за сваку димензију пора, при чему су ови коефицијенти ефективне дифузивности дистрибуирани на основу података о расподели величина пора. Симулацијом наткритичног сушења је потврђено да температура сушења и димензије гела имају значајан утицај на време сушења.

(Примљено 30. јуна 2003, ревидирано 6. јула 2004)

#### REFERENCES

1. D. W. Matson, R. D. Smith, *J. Am. Ceram. Soc.* **72** (1989) 871
2. J. Fricke, A. Emmerling, *J. Am. Ceram. Soc.* **75** (1992) 2027
3. G. W. Scherer, *J. Non-Cryst. Solids* **145** (1992) 33
4. T. Woignier, J. Phalippou, J. F. Quinson, M. Pauthe, F. Laveissiere, *J. Non-Cryst. Solids* **145** (1992) 25
5. B. C. Roy, M. Goto, T. Hirose, *Ind. Eng. Chem. Res.* **35** (1996) 607
6. M. Perrut, J. Y. Clavier, M. Poletto, E. Reverchon, *Ind. Eng. Chem. Res.* **36** (1997) 430
7. I. Goodarznia, M. H. Eikani, *Chem. Eng. Sci.* **53** (1998) 1387
8. E. Reverchon, M. Poletto, *Chem. Eng. Sci.* **51** (1996) 3741
9. E. Reverchon, C. Marrone, *Chem. Eng. Sci.* **52** (1997) 3421
10. C. Marrone, M. Poletto, E. Reverchon, A. Stassi, *Chem. Eng. Sci.* **53** (1998) 3711
11. M. P. Srinivasan, J. M. Smith, B. J. McCoy, *Chem. Eng. Sci.* **45** (1990) 1885
12. G. Madras, C. Thibaud, C. Erkey, A. Akgerman, *AIChE J.* **40** (1994) 777
13. L. Barna, J. M. Blanchard, E. Rauzy, C. Berro, P. Moszkowicz, *Chem. Eng. Sci.* **51** (1996) 3861
14. J. M. Moses, R. J. Willey, S. Rouanet, *J. Non-Cryst. Solids* **145** (1992) 41
15. M. J. van Bommel, A. B. de Haan, *J. Mat. Sci.* **29** (1994) 943
16. M. J. van Bommel, A. B. de Haan, *J. Non-Cryst. Solids* **186** (1995) 78
17. A. M. Orlović, Dj. T. Janačković, S. Drmanić, Z. Marinković, D. U. Skala, *J. Serb. Chem. Soc.* **66** (2001) 685
18. A. Orlović, Dj. Janačković, D. Skala, *Cat. Comm.* **3** (2002) 119
19. J. M. Miller, D. Wails, J. S. Hartman, J. L. Belelie, *J. Chem. Soc. Faraday Trans.* **93** (1997) 2439
20. R. M. M. Stevens, X. M. Shen, Th. W. de Loos, J. de Swaan Arons, *J. Supercritical Fluids* **11** (1997) 1
21. B. Carnahan, H. A. Luther, J. O. Wilkes, *Applied Numerical Methods*, Wiley, New York, 1969
22. R. C. Reid, J. M. Prausnitz, T. K. Sherwood, *The Properties of Gases and Liquids*, McGraw-Hill Book Company, New York, 1977
23. P. Capek, V. Hejtmanek, O. Solcova, K. Klusacek, P. Schneider, *Catal. Today* **38** (1997) 31
24. J. Gilron, A. Soffer, *J. Membr. Sci.* **209** (2002) 339
25. J. R. Katzer, in *Chemistry and Chemical Engineering of Catalytic Processes*, R. Prins and G.C.A. Schuit Eds., Sijthoff & Noordhoff, Alphen aan den Rijn, 1980 p. 49
26. X. Fang, D. J. Gunn, *Chem. Eng. Sci.* **51** (1996) 2673.